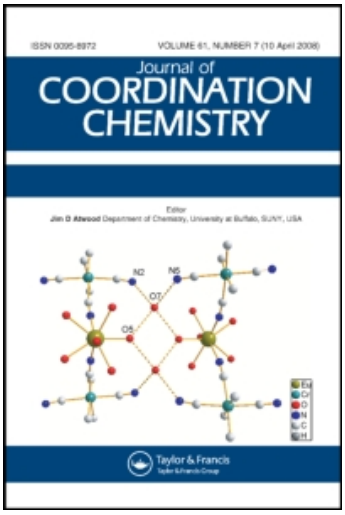

Journal of Coordination Chemistry
Publication details, including instructions for authors and subscription information:
http://www.informaworld.com/smpp/title~content=t713455674

Synthesis, structure, and DNA-binding of a new binuclear copper(II) complex: $[Cu_2(heap)(H_2O)_2](pic)_2 \cdot 2H_2O$

Xiao-Wei Zhang[a]; Yong-Jun Zheng[ab]; Yan-Tuan Li[a]; Zhi-Yong Wu[a]; Cui-Wei Yan[c]
[a] Marine Drug and Food Institute, Ocean University of China, Qingdao 266003, P.R. China [b] Department of Chemistry, Qufu Normal University, Qufu, Shandong 273165, P.R. China [c] College of Marine Life Science, Ocean University of China, Qingdao 266003, P.R. China

First published on: 03 August 2010

To cite this Article Zhang, Xiao-Wei , Zheng, Yong-Jun , Li, Yan-Tuan , Wu, Zhi-Yong and Yan, Cui-Wei(2010) 'Synthesis, structure, and DNA-binding of a new binuclear copper(II) complex: $[Cu_2(heap)(H_2O)_2](pic)_2 \cdot 2H_2O$', Journal of Coordination Chemistry, 63: 17, 2985 — 2998, First published on: 03 August 2010 (iFirst)
To link to this Article: DOI: 10.1080/00958972.2010.505647
URL: http://dx.doi.org/10.1080/00958972.2010.505647

Journal of Coordination Chemistry
Vol. 63, No. 17, 10 September 2010, 2985–2998

Synthesis, structure, and DNA-binding of a new binuclear copper(II) complex: $[Cu_2(heap)(H_2O)_2](pic)_2 \cdot 2H_2O$

XIAO-WEI ZHANG†, YONG-JUN ZHENG†‡, YAN-TUAN LI*†, ZHI-YONG WU† and CUI-WEI YAN*§

†Marine Drug and Food Institute, Ocean University of China, 5 Yushan Road, Qingdao 266003, P.R. China
‡Department of Chemistry, Qufu Normal University, Qufu, Shandong 273165, P.R. China
§College of Marine Life Science, Ocean University of China, 5 Yushan Road, Qingdao 266003, P.R. China

(*Received 9 December 2009; in final form 13 May 2010*)

In this study, a new μ-oxamido-bridged binuclear copper(II) complex $[Cu_2(heap)(H_2O)_2](pic)_2 \cdot 2H_2O$, where heap and pic stand for the anion of *N*,*N*′-*bis*(*N*-hydroxyethylaminopropyl)oxamide and 2,4,6-trinitrophenol, respectively, has been synthesized and characterized by elemental analyses, IR, UV, molar conductance, and single-crystal X-ray diffraction. The complex has an embedded inversion center at the middle of the C–C bond of the oxamido group. Each copper(II) is in a square-pyramidal coordination geometry. The bridging ligand (heap) adopts a *bis*-tetradentate *trans* conformation and the oxamido group is in an imidic acid configuration. Hydrogen bonds contribute to a 3-D supramolecular structure in the crystal. The interaction of the binuclear complex with herring sperm deoxyribonucleic acid (*HS*-DNA) has been investigated by using absorption and emission spectra, electrochemical techniques, and viscometry. The results suggest that the binuclear copper(II) complex interacts with *HS*-DNA by electrostatic interaction with intrinsic binding constant of 2.67×10^4 $(\text{mol L}^{-1})^{-1}$. The influence of anions on the structure and the interaction of the binuclear complex with *HS*-DNA were preliminarily discussed.

Keywords: Crystal structure; Binuclear copper(II) complex; μ-Oxamido-bridge; DNA interaction; 2,4,6-Trinitrophenol

1. Introduction

There is interest in the synthesis and interaction between transition metal complexes and deoxyribonucleic acid (DNA) as a fundamental requirement, not only for gaining insight into the reactive models for protein–nucleic acid interactions and probes of DNA structure, but also for obtaining information about drug design and tools of molecular biology [1–5]. Much effort has been devoted to the design and synthesis of copper(II) complexes because copper, a physiologically essential metal element, plays an important role in the endogenous oxidative DNA damage associated with aging and

*Corresponding authors. Email: yantuanli@ouc.edu.cn; cuiweiyan@ouc.edu.cn

Journal of Coordination Chemistry
ISSN 0095-8972 print/ISSN 1029-0389 online
DOI: 10.1080/00958972.2010.505647

cancer [6–12]. Compared with the number of studies dealing with mononuclear complexes, relatively few studies on binuclear copper(II) complexes have been reported [13–16]. However, the fact that a number of nucleases have two or three metal ions in their catalytic center [17] prompted us to design and synthesize new binuclear complexes to gain some insight into the DNA-binding properties of this kind of complex.

N,*N*′-*bis*(substituent)oxamides are good candidates as the binucleating bridging ligand in forming binuclear complexes because their coordinating ability toward transition–metal ions can be modified and tuned by changing the nature of the amide substituents [18, 19]. A series of binuclear complexes with interesting structures based on the bridging *N*,*N*′-*bis*(substituent)oxamides along with their magnetic properties have been reported [20, 21]. However, studies on DNA-binding properties of such complexes are limited [22].

With these facts in mind and in continuation of our work on the syntheses and properties of complexes with oxamido-bridges [12, 23–27], in this article we chose *N*,*N*′-*bis*(*N*-hydroxyethylaminopropyl)oxamide (heap) as bridging ligand and picrate anion (pic) as counterion to synthesize a new μ-oxamido-bridged binuclear copper(II) complex $[Cu_2(heap)(H_2O)_2](pic)_2 \cdot 2H_2O$, and the crystal structure of the complex has been solved by single-crystal X-ray diffraction. The interaction of the binuclear complex with herring sperm DNA (*HS*-DNA) has been studied to examine the influence of counterions on structure and DNA-binding properties.

2. Experimental

2.1. *Materials*

The *N*,*N*′-*bis*(*N*-hydroxyethylaminopropyl)oxamide (H_2heap) and $Cu(pic)_2 \cdot 6H_2O$ were synthesized according to the reported method [18, 28]. Ethidium bromide (EB) and *HS*-DNA were purchased from Sigma Corporation and used as received. All other reagents used in the synthesis were of analytical grade.

2.2. *Synthesis of* $[Cu_2(heap)(H_2O)_2](pic)_2 \cdot 2H_2O$

A 6 mL methanol solution of 62.7 mg (0.1 mmol) $Cu(pic)_2 \cdot 6H_2O$ was added dropwise to a methanol (6 mL) solution containing H_2heap (14.5 mg, 0.05 mmol) and piperidine (8.5 mg, 0.1 mmol). The mixture was heated under reflux with stirring at 323 K for 4 h. The resulting green solution was filtered and then an equal volume of water was added. Green crystals suitable for X-ray analysis were obtained from the solution after 5 days by slow evaporation at room temperature. Yield, 20.8 mg (44%). Anal. Calcd for $Cu_2C_{24}H_{36}N_{10}O_{22}$ (%): C, 30.55; H, 3.85; N, 14.84. Found (%): C, 30.28; H, 3.73; N, 14.97.

2.3. *Physical measurements*

The C, H, and N microanalyses were performed on a Perkin-Elmer 240 elemental analyzer. Molar conductance was measured with a Shanghai DDS-11A conductometer.

Infrared spectra were recorded on a Nicolet-470 spectrophotometer from 4000 to 400 cm^{-1} as KBr pellets. The UV-Vis spectrum was recorded in a 1-cm path length quartz cell on a Cary 300 spectrophotometer. Fluorescence was tested on a Fp-750w fluorometer. Cyclic voltammetric experiments were carried out using a CHI 832B electrochemical analyzer in connection with a glassy carbon working electrode (GCE), saturated calomel reference electrode (SCE), and a platinum wire auxiliary electrode.

2.4. *Crystal structure determination*

The X-ray diffraction experiment for complex was made on a Bruker diffractometer with graphite monochromatic radiation ($\lambda = 0.71073$ Å). The crystal structure was solved by direct methods followed by Fourier syntheses. Structure refinement was performed by full-matrix least-squares (SHELXL-97) on F^2 [29]. All hydrogens were located in a difference Fourier map; those on oxygen were included in the structure-factor calculation in riding mode with refined displacement parameters. Other hydrogens were refined freely. Crystal data are summarized in table 1.

2.5. *DNA binding studies*

All experiments involving *HS*-DNA were performed in Tris-HCl buffer solution (pH = 7.24), prepared using deionized and sonicated triply distilled water. Solutions of *HS*-DNA in Tris-HCl gave a ratio of UV absorbance at 260 and 280 nm, A_{260}/A_{280}, of ≈1.9, indicating that the DNA was sufficiently free of protein [30]. The concentration of *HS*-DNA was determined by UV absorbance at 260 nm. The extinction coefficient,

Table 1. Crystal data and details of the structure determination of $[Cu_2(heap)(H_2O)_2](pic)_2 \cdot 2H_2O$.

Empirical formula	$C_{24}H_{36}Cu_2N_{10}O_{22}$
Formula weight	943.73
Crystal system	Monoclinic
Space group	$P2(1)/n$
Unit cell dimension (Å, °)	
a	15.454(3)
b	6.8510(14)
c	17.360(4)
α	90.00
β	92.59(3)
γ	90.00
Volume (Å^3), Z	1836.1(6), 2
Calculated density (g cm^{-3})	1.707
Absorption coefficient μ (Mo-Kα) (mm^{-1})	1.260
Scan-mode	φ and ω scan
F(000)	968
Crystal size (mm^3)	$0.15 \times 0.18 \times 0.21$
θ range for data collection (°)	1.81−27.62
Limiting indices	$-20 < h < 20$; $-8 < k < 8$; $-18 < l < 22$
Total, unique data	34,290, 4244, [R(int) = 0.0175]
Observed data [$I > 2\sigma(I)$]	3918
R, wR_2	0.0251, 0.0682
S	1.059
Maximum average shift/error	0.00, 0.00

$\varepsilon 260$, was taken as 6600 L mol^{-1} cm^{-1} [31]. Stock solution of DNA was stored at 277 K and used after not more than 4 days. Concentrated stock solution of the binuclear copper(II) complex was prepared by dissolving the complex in Tris-HCl buffer to required concentrations for all the experiments. Absorption spectral titration experiment was performed by keeping the concentration of the copper(II) complex constant while varying the *HS*-DNA concentration. Equal solution of *HS*-DNA was added to the copper(II) complex solution and reference solution to eliminate absorbance of DNA itself. In the EB fluorescence displacement experiment, 5 μL of the EB Tris-HCl solution (1.0 mmol L^{-1}) was added to 1 mL of DNA solution (at saturated binding levels [32]) and stored in the dark for 2 h. Then, the solution of the copper(II) complex was titrated into the DNA/EB mixture and diluted in Tris-HCl buffer to 5 mL, producing the solutions with the varied mole ratio of the copper(II) complex to *HS*-DNA. Before measurements, the mixture was shaken and incubated at room temperature for 30 min. The fluorescence spectra of EB bound to *HS*-DNA were obtained at an emission wavelength of 584 nm in the Fluorometer. The electrochemical titration experiments were performed by keeping the concentration of the complex constant while varying the *HS*-DNA concentration using the solvent of Tris-HCl buffer. Viscosity measurement was carried out using an Ubbelodhe viscometer immersed in a thermostatic water bath maintained at 289(±0.l) K. DNA samples approximately 200 base pairs in length were prepared by sonication to minimize complexities arising from DNA flexibility [33]. Flow times were measured with a digital stopwatch, and each sample was measured three times, and an average flow time was calculated. Relative viscosities for *HS*-DNA in the presence and absence of the complex were calculated from the relation $\eta = (t - t_0)/t_0$, where t is the observed flow time of DNA-containing solution and t_0 is that of Tris-HCl buffer alone. Data were presented as $(\eta/\eta_0)^{1/3}$ *versus* binding ratio [34], where η is the viscosity of DNA in the presence of the complex and η_0 is the viscosity of DNA alone.

3. Results and discussion

3.1. *General properties of the complex*

The copper(II) complex is more soluble in water, DMF and DMSO giving stable solutions at room temperature; whereas, it is moderately soluble in methanol and acetone, and practically insoluble in carbon tetrachloride, chloroform, and benzene. In the solid state, the complex is stable in air so as to allow physical measurements. The molar conductance value (132 Ω^{-1} cm^{-2} mol^{-1}) of the binuclear copper(II) complex in DMF solution falls in the expected range for 1 : 2 electrolytes [35], suggesting that the two picrate anions in complex are situated outside the metal coordination sphere. The results coincide with the following spectroscopic data.

3.2. *IR spectrum*

In the IR spectrum of the complex, the N–H and O–H vibrations of the bridging ligand (H_2heap) appear in the region 3300–3000 cm^{-1} and the carbonyl stretching vibration at 1700 cm^{-1} for H_2 heap is considerably red shifted to 1634 cm^{-1} in the binuclear

complex, indicating that the oxygens of C=O take part in coordination to copper(II) [36]. In addition, free Hpic has $\upsilon_{as}(NO_2)$ at 1555 cm^{-1} and $\upsilon_s(NO_2)$ at 1342 cm^{-1}, respectively. In the binuclear complex, $\upsilon_{as}(NO_2)$ of pic^- emerges at 1567 cm^{-1}, and $\upsilon_s(NO_2)$ of pic^- splits into two bands at 1344 and 1365 cm^{-1}, suggesting that the nitryl oxygens of pic^- take no part in coordination [37].

3.3. *Electronic spectrum*

The electronic spectrum of the complex was recorded in the UV-Vis region (200–800 nm). Three absorptions with varied intensity can be observed. The intense band at 220 nm is assigned to intra-ligand (π–π^*) transition associated with picrate, while the less intense band around 352 nm corresponds to charge transfer transition between the picrate and metals [38]. Besides, the broad band observed at the lower frequency of 638 nm matches well with the reported d–d transition of five-coordinate square-pyramidal copper(II) [39].

The spectroscopic data of the copper(II) complex are in agreement with the following determination of the crystal structure.

3.4. *Crystal structure*

As shown in figure 1, the structure of $[Cu_2(heap)(H_2O)_2](pic)_2 \cdot 2H_2O$ consists of a centrosymmetric dinuclear copper(II) complex cation $[Cu_2(heap)(H_2O)_2]^{2+}$, two picrate anions, and two lattice waters. Copper(II) has square-pyramidal coordination, with four atoms (N1, N2, $O1^i$, O2) (symmetry code: (^{i}) $1-x$, $1-y$, $1-z$) from the oxamide ligand in the basal plane and one water (O10) at the apical position. Cu1 displaces 0.2271(7) Å from the basal plane. The apical Cu–O distance of 2.2628(14) Å is significantly longer than those in the basal plane (table 2). In accordance with the donor abilities, the sp^2 hybrid N1 has a shorter Cu–N bond [1.9438(13) Å] than the sp^3 hybrid N2 [1.9797(13) Å] [40].

The deprotonated oxamido bridging ligand adopts a *bis*-tetradentate *trans* conformation with an inversion center at the mid-point of the C1–$C1^i$ bond. It forms two five- and one six-membered chelate rings around each copper(II). The five-membered Cu1–N1–C1–$C1^i$–$O1^i$ (symmetry code: (^{i}) $1-x$, $1-y$, $1-z$) ring is almost planar, whereas the other Cu1–N2–C5–C6–O2 takes on a twist conformation with the puckering parameters of $Q = 0.432(2)$ Å, and $\varphi = 90.32(16)^\circ$. The six-membered Cu1–N1–C2–C3–C4–N2 cycle is intermediate between half-chair and screw-boat conformations with the puckering parameters of $Q = 0.568(2)$ Å, $\varphi = 212.6(2)^\circ$, and $\theta = 55.22(16)^\circ$. The oxamido bridge is planar as observed in other oxamido-bridged copper(II) complexes [12, 41–43] and the Cu···Cu separation [44–46] within the binuclear unit is 5.1769(10) Å.

In the picrate, the *para*-nitro group is almost coplanar with the linked phenyl ring, but both *ortho*-nitro groups are non-coplanar with the benzene plane; the dihedral angles are 20.6(2)° (N3O4O5), and 39.01(11)° (N5O8O9). For C7 and C1, both are sp^2 carbons, comparing the bond lengths of C7–O3 and C1–O1 is interesting, 1.253(2) Å *versus* 1.2759(18) Å, which implies that C1–O1 is a single bond as C7–O3 and O1 atom has a negative charge. The 0.023(3) Å longer of C1–O1 can be attributed to coordination of O1 with Cu1. Furthermore, C1–N1 is 1.2945(19) Å, a typical C=N

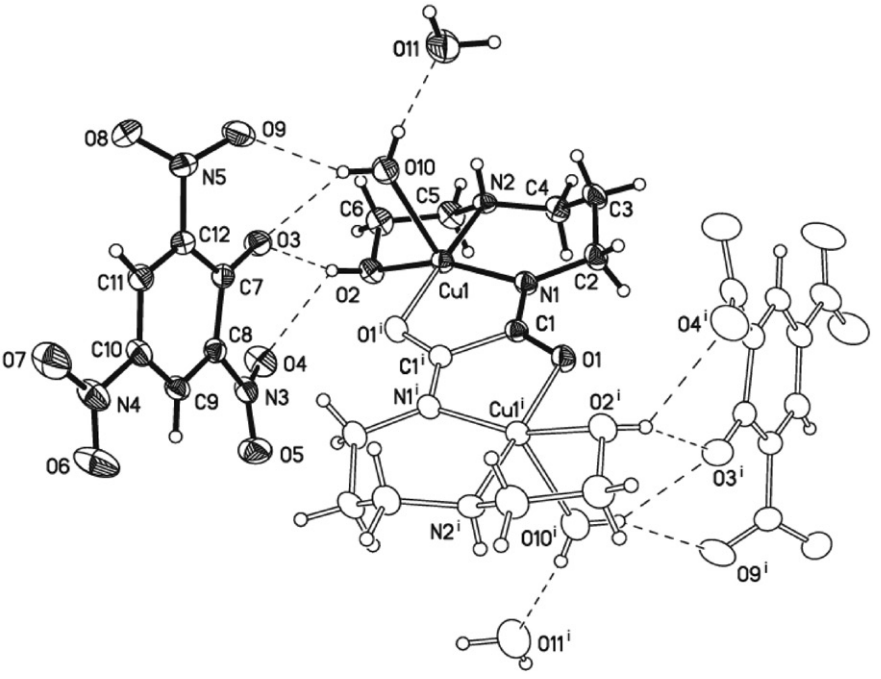

Figure 1. A view of $[Cu_2(heap)(H_2O)_2](pic)_2 \cdot 2H_2O$ with the atom numbering scheme and thermal ellipsoids at 30% probability. The dashed lines indicate hydrogen bonds. (Symmetry code: (^{i}) $1-x$, $1-y$, $1-z$).

Table 2. Selected bond distances (Å) and angles (°) for $[Cu_2(heap)(H_2O)_2](pic)_2 \cdot 2H_2O$.

Cu1–N1	1.9438(13)	C1–C1^i	1.517(3)
Cu1–N2	1.9797(13)	C1–N1	1.2945(19)
Cu1–O1^i	1.9612(11)	C1–O1	1.2759(18)
Cu1–O2	2.0076(12)	C7–O3	1.253(2)
Cu1–O10	2.2628(14)		
N1–Cu1–N2	96.82(6)	N2–Cu1–O1^i	173.99(5)
N1–Cu1–O1^i	85.41(5)	N2–Cu1–O10	90.83(6)
N1–Cu1–O2	158.44(5)	O1^i–Cu1–O2	91.36(5)
N1–Cu1–O10	111.06(6)	O1^i–Cu1–O10	93.59(5)
N2–Cu1–O2	84.52(5)	O2–Cu1–O10	90.39(6)

Symmetry code: ^i1-x, $1-y$, $1-z$.

double bond value. Hence, the oxamide group adopts the imidic acid conformation and is deprotonated at O1.

Hydrogen bonds lead to formation of a 3-D supramolecular framework. As shown in figure 2, a couple of lattice water molecules (O11) and picrates form a circular hydrogen bonding dimer. These dimers and complex cations $[Cu_2(heap)(H_2O)_2]^{2+}$ arrange by turns along the *a*-axis to form a 1-D chain through the hydrogen bonds (table 3) between the complex cations and picrate anions. These chains are assembled by the hydrogen bonds between coordination water (O10) and lattice water (O11) to complete a 3-D supramolecular structure (figure 3). In addition, a weaker N–H···O and two C–H···O hydrogen bonds contribute to the assembly of the chains.

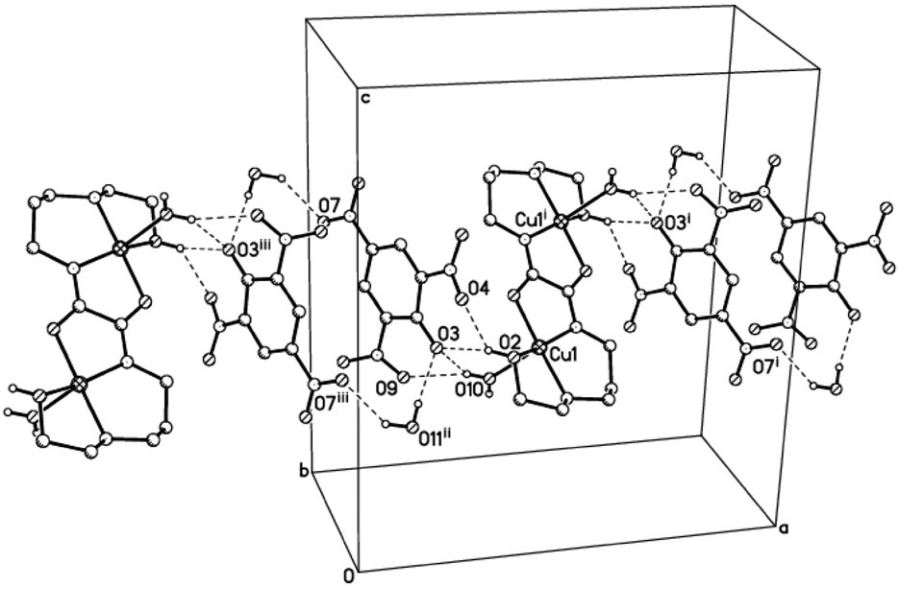

Figure 2. The 1-D chain extending in the *a* direction. Hydrogens not involved in hydrogen bonding have been omitted for clarity. Hydrogen bonds are shown as dotted lines (Symmetry codes: (i) $1-x, 1-y, 1-z$; (ii) $1/2-x, y-1/2, 1/2-z$; (iii) $-x, 1-y, 1-z$).

Table 3. Distances (Å) and angles (°) of the hydrogen bonds for $[Cu_2(heap)(H_2O)_2](pic)_2 \cdot 2H_2O$.

D–H···A	*d*(D–H)	*d*(H···A)	*d*(D···A)	∠(D–H···A)
O2–H2···O3	0.88	1.82	2.667(2)	161
O2–H2···O4	0.88	2.36	2.895(2)	119
O10–H10A···O11	0.81	1.93	2.738(2)	171
O10–H10B···O3	0.82	2.40	3.014(2)	132
O10–H10B···O9	0.82	2.19	2.961(2)	155
O11–H11A···O3^{iv}	0.86	1.99	2.832(2)	163
O11–H11B···O7^{v}	0.97	2.14	2.980(3)	145
N2–H2C···O8^{ii}	0.83(2)	2.45(2)	3.188(2)	149.1(17)
C4–H4B···O6^{vi}	0.93(2)	2.54(2)	3.460(3)	173.6(16)
C11–H11···O7^{vii}	0.90(2)	2.57(2)	3.462(3)	172.1(18)

Symmetry codes: $^{ii}1/2-x, y-1/2, 1/2-z$; $^{iv}1/2-x, y+1/2, 1/2-z$; $^{v}x+1/2, 3/2-y, z-1/2$; $^{vi}1/2+x, 1/2-y, z-1/2$; and $^{vii}-x, 2-y, 1-z$.

If we compare the crystal structure of the complex used in this study with that of previously reported analogous complex $[Cu_2(heap)(NO_3)_2]$ [12], we find that the two complexes have the same skeletal structure. Copper(II) coordination environments in both the complexes are square pyramidal, and both crystallize in monoclinic form. The main difference between $[Cu_2(heap)(H_2O)_2](pic)_2 \cdot 2H_2O$ and $[Cu_2(heap)(NO_3)_2]$ is that the picrate anion and water molecules in the former case and nitrate group in the latter result in two differences between the two complexes. The first difference is the space groups ($P2(1)/n$ for the former and $P2(1)/c$ for the latter). The second difference is that the former contains a $[Cu_2(heap)(H_2O)_2]^{2+}$ cation in the solid while the latter is neutral.

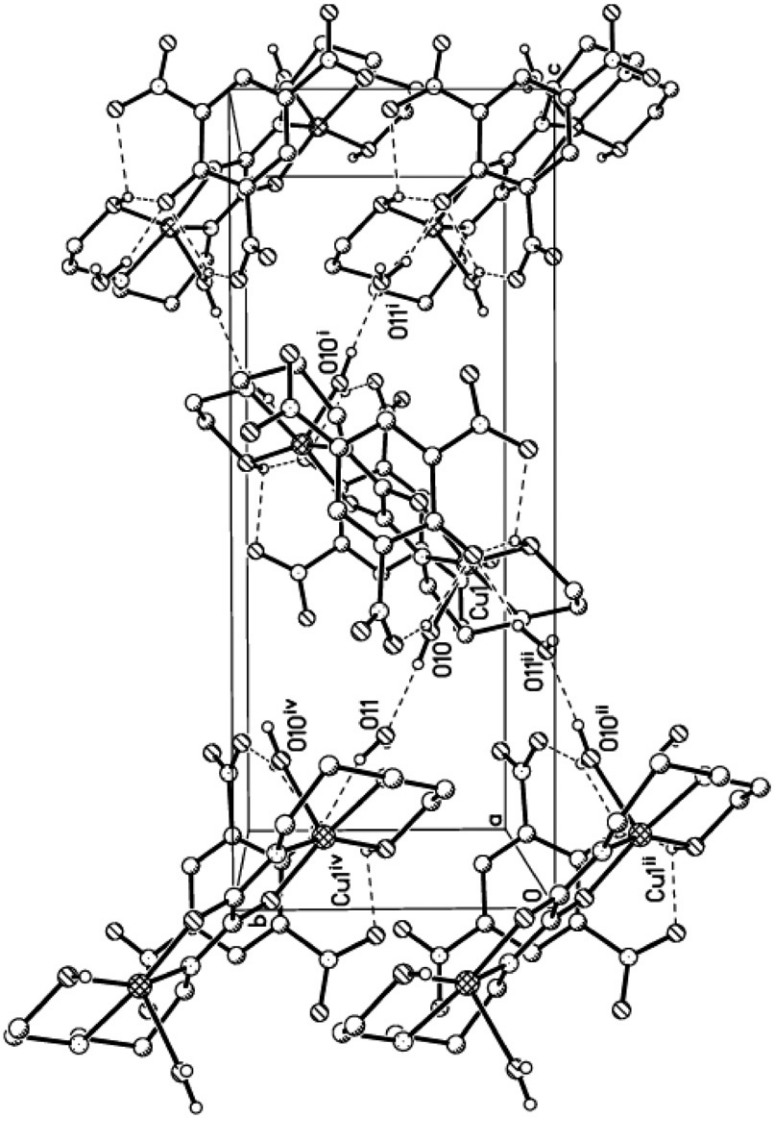

Figure 3. Hydrogen bonds between coordination water (O10) and lattice water (O11) link the chains in figure 2 to form a 3-D structure (Symmetry codes: (i) $1-x, 1-y, 1-z$; (ii) $1/2-x, y-1/2, 1/2-z$; (iv) $1/2-x, y+1/2, 1/2-z$).

Furthermore, the difference of the counterions in the two complexes also has effects on the DNA-binding properties (*vide infra*).

3.5. *DNA-binding studies*

3.5.1. Electronic absorption titration. Electronic absorption spectroscopy is an effective method to examine the binding modes and magnitudes of metal complexes with DNA [47]. The absorption spectra of the copper(II) complex in the absence and presence of *HS*-DNA are given in figure 4. When titrated by *HS*-DNA, the band of the complex at 220 nm presented hypochromism of about 14% at a ratio of [DNA]/[complex] of 8 and shows no red shift. Such characteristics of UV is similar to $[Ru(tpy)(PHBI)](ClO_4)_2 \cdot 2H_2O$ [48], which is interpreted as electrostatic interaction with DNA. Thus, this observation leads us to suspect that the copper(II) complex may interact with DNA through electrostatic binding.

To quantitatively evaluate the binding magnitude of the copper(II) complex with *HS*-DNA, the intrinsic binding constant K_b was determined by monitoring the changes in absorbance at 220 nm using the following equation [49]:

$$[\mathrm{DNA}]/(\varepsilon_a - \varepsilon_f) = [\mathrm{DNA}]/(\varepsilon_b - \varepsilon_f) + 1/\left[K_b(\varepsilon_b - \varepsilon_f)\right], \quad (1)$$

where [DNA] is the concentration of *HS*-DNA and ε_a, ε_f, and ε_b correspond to the extinction coefficient, respectively, for each addition of DNA to the copper(II) complex, for the free copper(II) complex, and for the copper(II) complex in the fully bound form. From the $[\mathrm{DNA}]/(\varepsilon_a - \varepsilon_f)$ *versus* [DNA] plot (inset in figure 4), the binding constant K_b for the copper(II) complex was estimated to be $2.67 \times 10^4 (\mathrm{mol\,L^{-1}})^{-1}$ ($R = 0.9907$ for 5-points), lower than those of typical intercalators (e.g., EB–DNA, $\sim 10^6 (\mathrm{mol\,L^{-1}})^{-1}$)

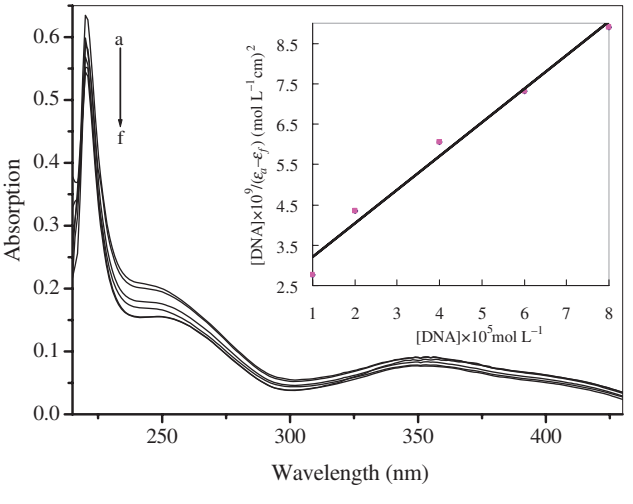

Figure 4. Electronic absorption spectra of the copper(II) complex upon titration of *HS*-DNA. [complex] = $1.0 \times 10^{-5}\,\mathrm{mol\,L^{-1}}$; [DNA]/[complex]: (a) 0, (b) 1, (c) 2, (d) 4, (e) 6, (f) 8. Arrow indicates the change upon increasing the DNA concentrations. Inset: Plot of $[\mathrm{DNA}]/(\varepsilon_a - \varepsilon_f)$ *vs.* [DNA] for the absorption titration of *HS*-DNA with the copper(II) complex.

[50], but higher than those of mononuclear copper(II) complexes $[Cu(C_{24}H_{40}N_4)_2Br](ClO_4)_5 \cdot 2H_2O$ and $[Cu(C_{36}H_{64}N_4)_2Br](ClO_4)_5 \cdot H_2O$ [8]. The hypochromism with no red shift and the low K_b value indicate that the interaction between the dicopper(II) complex and *HS*-DNA is different from classical intercalation. Considering the structure of the dicopper(II) complex and the results of $[Ru(tpy)(PHBI)](ClO_4)_2 \cdot H_2O$ [48] interacting with DNA-binding, we speculate that the dicopper(II) complex may facilitate the electrostatic interaction when interacting with *HS*-DNA in Tris-HCl buffer. Hypochromism may be due to the positively charged binuclear copper(II) complex cation $[Cu_2(heap)(H_2O)_2]^{2+}$ electrostatic binding to negatively charged phosphate backbone at the periphery of the double helix *HS*-DNA, which resulted in *HS*-DNA contraction and conformation changing [51]. This view is supported by EB fluorescence displacement experiments, cyclic voltammetric studies, and viscosity measurements (*vide infra*).

3.5.2. The EB fluorescence displacement experiments. To further investigate the interaction mode between copper(II) and *HS*-DNA, EB fluorescence displacement experiments were also employed. The intrinsic fluorescence intensity of DNA is very low and that of EB in Tris-HCl buffer is also not high due to the quenching by solvent. However, on addition of DNA, the fluorescence intensity of EB is enhanced because of its intercalation into the DNA. Thus, EB can be used to probe the interaction of complexes with DNA. The fluorescence intensity of EB can be quenched by the addition of another molecule due to the displacement of EB from DNA [52]. In our experiment, as depicted in figure 5, the fluorescence intensity of EB at 584 nm shows a remarkable decreasing trend with the increasing concentration of the complex, suggesting that the dicopper(II) complex binds strongly with *HS*-DNA. The quenching

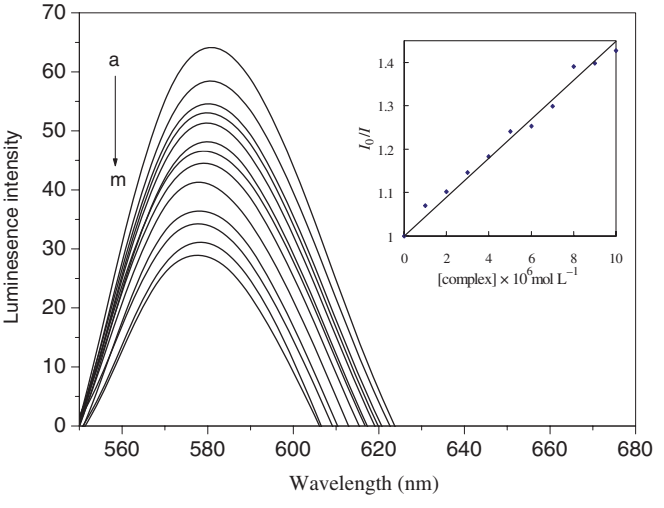

Figure 5. Emission spectra of the *HS*-DNA-EB system upon titration of the copper(II) complex. Arrow shows the change upon increasing complex concentration. Inset: Plot of I_0/I *vs.* [complex] for the titration of the copper(II) complex to *HS*-DNA–EB system.

of EB bound to the DNA by complex is in agreement with the linear Stern–Volmer equation [53]:

$$I_0/I = 1 + K_{sv}[Q], \tag{2}$$

where I_0 and I represent the fluorescence intensities in the absence and presence of quencher, respectively. K_{sv} is a linear Stern–Volmer quenching constant and Q is the concentration of quencher (in this article, quencher denotes complex). In the quenching plot of I_0/I *versus* [complex], K_{sv} is given by the ratio of the slope to intercept. The K_{sv} value for the complex is 4.48×10^4 ($R = 0.9921$ for 10-points).

3.5.3. Cyclic voltammetric studies. The application of the cyclic voltammetric technique to study the interaction between metal complexes and DNA provides a useful complement to the previously used spectral studies [54]. In this study, it is employed to understand the nature of the DNA-binding of the copper(II) complex, and the result is shown in figure 6. At a scan rate of 0.20 V s^{-1}, in the absence of *HS*-DNA (curve a), the copper(II) complex shows two couples [couple 1: −0.429 V (E_{pc1}) and −0.104 V (E_{pa1}); couple 2: −0.780 V (E_{pc2}) and −0.586 V (E_{pa2})] which may correspond to Cu(II)Cu(II)/Cu(I)Cu(II) and Cu(I)Cu(II)/Cu(I)Cu(I), respectively. The separations of anodic and cathodic peak (ΔE_p) for couples 1 and 2 are 0.325 V and 0.194 V, respectively. The formal potentials of couples 1 and 2 in free form ($E_f^{o'}$), taken as the average of E_{pc} and E_{pa}, are −0.267 V and −0.683 V, respectively. In the presence of *HS*-DNA (curve *b*), couple 2 disappears. The formal potential of couple 1 [−0.462 V (E_{pc1}) and −0.104 V (E_{pa1})] shifts to more negative potential ($\Delta E'_o = E_b^{o'} - E_f^{o'} = -0.016$ V) and the voltammetric peak currents decrease. The shift to negative in E'_o indicates that the interaction mode between the complex and *HS*-DNA is electrostatic [55]. The changes in the peak currents can be attributed to increased difficulty in diffusion of the

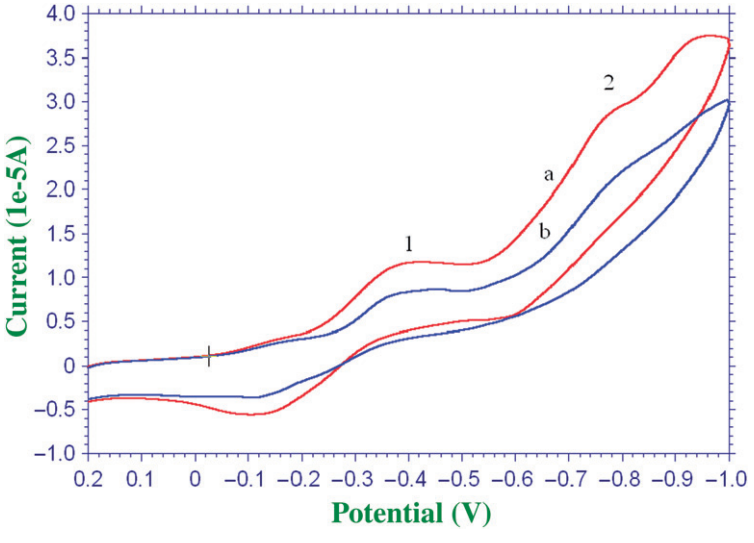

Figure 6. Cyclic voltammograms of $[Cu_2(heap)(H_2O)_2](pic)_2 \cdot 2H_2O$ in the absence (a) and presence (b) of *HS*-DNA.

dicopper(II) complex bound to the large, slowly diffusing *HS*-DNA molecule [56]. The separation between $E_b^{o'}$ and $E_f^{o'}$ can be used to estimate the ratio of binding constants for the reduced and oxidized forms to DNA using the equation [57]:

$$E_b^{o'} - E_f^{o'} = 0.059 \log[K_R/K_O], \quad (3)$$

where K_R and K_O are the binding constants of reduced and oxidized forms to DNA, respectively. The ratio of constants for the binding of the $K_{Cu(I)Cu(II)}$ and $K_{Cu(II)Cu(II)}$ ions to *HS*-DNA was estimated to be 0.54 for the complex, suggesting that the Cu(II)Cu(II) form of the complex interacts more strongly than the Cu(I)Cu(II) form.

3.5.4. Viscosity measurements. Viscosity measurement, which is sensitive to changes in the length of DNA, is regarded as the least ambiguous and most critical means of studying the binding mode of metal complexes with DNA in solution and provides stronger arguments for intercalative-binding mode [58, 59]. To further clarify the interaction mode of the copper(II) complex and *HS*-DNA, the viscosity measurement was carried out. As illustrated in figure 7, on increasing the amount of the binuclear complex, the relative viscosity of *HS*-DNA is essentially unchanged, very similar to that observed for other complexes which interacted with DNA in electrostatic mode [48]. Thus, the viscosity measurement is consistent with the results of the electronic absorption titrations, EB fluorescence displacement experiments, and cyclic voltammetric studies.

From the experiment evidence we speculate that the interaction between the dicopper(II) complex and DNA is electrostatic, occurring between the positive charge in the complex and the negative phosphate backbone of *HS*-DNA [51, 60].

Comparing K_b and K_{sv} of $[Cu_2(heap)(H_2O)_2](pic)_2 \cdot 2H_2O$ (K_b, 2.67×10^4 $(mol\,L^{-1})^{-1}$; K_{sv}, 4.48×10^4) with that of complex $Cu_2(heap)(NO_3)_2$ (K_b, 3.33×10^4 $(mol\,L^{-1})^{-1}$; K_{sv}, 2.01×10^5) [12], we find that both K_b and K_{sv} of the former are smaller than that of the latter, attributed to the dimensions of the picrate anions being larger than that of nitrate, which increases the steric hindrance between the positive charge $[Cu_2(heap)]^{2+}$ and the negative phosphate backbone of *HS*-DNA. These results confirm that structure

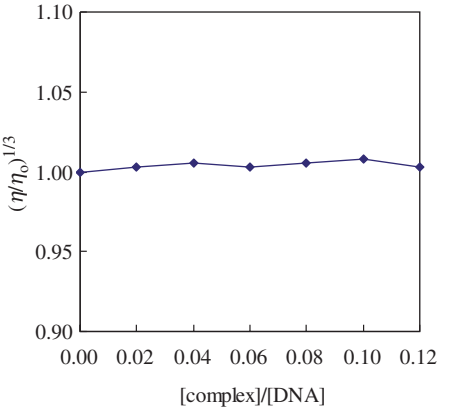

Figure 7. Effect of the increasing amount of the complex on the relative viscosity of *HS*-DNA at 289(±0.1) K, [DNA] = 0.2 mmol L^{-1}.

and affinity of the complex toward *HS*-DNA may be modified by changing the dimensions of the anions. This strategy should be valuable in designing structures and understanding the binding properties between the complexes and DNA.

Further investigations using various bridging ligands and counterions are still required in order to confirm this effect and are in progress in our laboratory.

Supplementary material

Crystallographic data have been deposited at the Cambridge Crystallographic Data Centre with the deposition numbers 730780. These data can be obtained free of charge *via* www.ccdc.ac.uk/conts/retrieving.html or from the Cambridge Crystallographic Centre, 12 Union Road, Cambridge CB2 1EZ, UK, Fax (+44)1223 336033, or E-mail: deposit@ccdc.cam.ac.uk.

Acknowledgments

This project was supported by the National Natural Science Foundation of China, the Natural Science Foundation of Qingdao City (No. 09-1-3-73-jch) and the PhD Program Foundation of Ministry of Education of China.

References

[1] S.J. Lippard. *Chem. Rev.*, **99**, 2467 (1999).
[2] K.E. Erkkila, D.T. Odom, J.K. Barton. *Chem. Rev.*, **99**, 2777 (1999).
[3] H.T. Chifotides, K.R. Dunbar. *Acc. Chem. Res.*, **38**, 146 (2005).
[4] B. Armitage. *Chem. Rev.*, **98**, 1171 (1998).
[5] W.K. Pogozelski, T.D. Tullius. *Chem. Rev.*, **98**, 1089 (1998).
[6] B.N. Ames, M.K. Shigenaga, T.M. Hagen. *Proc. Natl Acad. Sci.*, **90**, 7622 (1993).
[7] M. Jiang, Y.T. Li, Z.Y. Wu, Z.W. Yin. *J. Coord. Chem.*, **62**, 380 (2009).
[8] J.H. Li, J.T. Wang, L.Y. Zhang, Z.N. Chen, Z.W. Mao, L.N. Ji. *J. Coord. Chem.*, **62**, 1775 (2009).
[9] Y.Y. Kou, J.L. Tian, D.D. Li, H. Liu, W. Gu, S.P. Yan. *J. Coord. Chem.*, **62**, 2182 (2009).
[10] N. Raman, T. Jeyamurugan. *J. Coord. Chem.*, **62**, 2375 (2009).
[11] C.Y. Zhu, Y.T. Li, Z.Y. Wu, Y.L. Song. *J. Coord. Chem.*, **60**, 465 (2007).
[12] Y.T. Li, C.Y. Zhu, Z.Y. Wu, M. Jiang, C.W. Yan. *J. Coord. Chem.*, **62**, 3795 (2009).
[13] J.Z. Wu, L. Yuan, J.F. Wu. *J. Inorg. Biochem.*, **99**, 2211 (2005).
[14] Y.P. Li, Y.B. Wu, J. Zhao, P. Yang. *J. Inorg. Biochem.*, **101**, 283 (2007).
[15] Q.Q. Zhang, F. Zhang, W.G. Wang, X.L. Wang. *J. Inorg. Biochem.*, **100**, 1344 (2006).
[16] F. Zhang, Q.Q. Zhang, W.G. Wang, X.L. Wang. *J. Photochem. Photobiol., A: Chem.*, **184**, 241 (2006).
[17] W.N. Lipscomb, N. Sträter. *Chem. Rev.*, **96**, 2375 (1996).
[18] H. Ojima, K. Nonoyama. *Coord. Chem. Rev.*, **92**, 85 (1988).
[19] R. Ruiz, J. Faus, F. Lloret, M. Julve, Y. Journaux. *Coord. Chem. Rev.*, **193–195**, 1069 (1999).
[20] Y.T. Li, C.W. Yan, Z.Y. Wu, C.Y. Zhu. *J. Magn. Magn. Mater.*, **292**, 418 (2005).
[21] Z.L. Liu, L.C. Li, D.Z. Liao, Z.H. Jiang, S.P. Yan. *Cryst. Growth Des.*, **5**, 781 (2005).
[22] Z.Q. Liu, Y.T. Li, Z.Y. Wu, Y.L. Song. *Inorg. Chim. Acta*, **361**, 226 (2008).
[23] Y.T. Li, C.W. Yan, J. Zhang. *Cryst. Growth Des.*, **4**, 481 (2003).
[24] Y.T. Li, C.W. Yan, S.H. Miao, D.Z. Liao. *Polyhedron*, **17**, 2491 (1998).
[25] Y.T. Li, C.W. Yan, H.S. Guan. *Synth. Met.*, **144**, 69 (2004).
[26] Y.T. Li, C.Y. Zhu, G.Q. Li, C.W. Yan, G.Y. Xu. *Transition Met. Chem.*, **30**, 850 (2005).
[27] Y.T. Li, Z.Q. Liu, Z.Y. Wu, M. Jiang, X.W. Li. *Struct. Chem.*, **19**, 819 (2008).

[28] B.M. Ji, Z.X. Zhou, K.L. Ding, Y.Z. Li. *Polyhedron*, **17**, 4327 (1998).
[29] G.M. Sheldrick. *SHSLXL-97, Program for Crystal Structure Refinement*, University of Göttingen, Germany (1997).
[30] J. Marmur. *J. Mol. Biol.*, **3**, 208 (1961).
[31] M.E. Reichmann, S.A. Rice, C.A. Thomas, P.J. Doty. *J. Am. Chem. Soc.*, **76**, 3047 (1954).
[32] J.K. Barton, J.M. Goldberg, C.V. Kumar, N.J. Turro. *J. Am. Chem. Soc.*, **108**, 2081 (1986).
[33] J.B. Chaires, N. Dattagupta, D.M. Crothers. *Biochemistry*, **21**, 3933 (1982).
[34] G. Cohen, H. Eisenberg. *Biopolymers*, **8**, 45 (1969).
[35] W.J. Geary. *Coord. Chem. Rev.*, **7**, 81 (1971).
[36] K. Nakamoto. *Infrared and Raman Spectra of Inorganic and Coordination Compounds*, 5th Edn, Wiley, New York (1997).
[37] S.X. Liu, W.S. Liu, M.Y. Tan, K.B. Yu. *J. Coord. Chem.*, **39**, 105 (1996).
[38] M. Bourgoin, K.H. Wong, J.Y. Hui, J. Smid. *J. Am. Chem. Soc.*, **97**, 3462 (1975).
[39] P. Camurlu, A. Yilmaz, L. Tatar, D. Kısakürek, D. Ülkü. *Cryst. Res. Technol.*, **40**, 271 (2005).
[40] J.K. Tang, Y. Ou-Yang, H.B. Zhou, Y.Z. Li, D.Z. Liao, Z.H. Jiang, S.P. Yan, P. Cheng. *Cryst. Growth Des.*, **5**, 813 (2005).
[41] J.F. Lou, Y.T. Li, Z.Y. Wu, D.Q. Wang, J.M. Dou. *Acta Crystallogr.*, **C61**, m400 (2005).
[42] F. Sun, Y.T. Li, Z.Y. Wu, Y.L. Song, M. Jiang. *Acta Crystallogr.*, **C62**, m584 (2006).
[43] F. Lloret, M. Julve, J. Faus, Y. Journaux, M. Philoche-Levisalles, Y. Jeannin. *Inorg. Chem.*, **28**, 3702 (1989).
[44] D. Saravanakumar, N. Sengottuvelan, V. Narayanan, M. Kandaswamy, K. Chinnakali, G. Senthilkumar, H.K. Fun. *Eur. J. Inorg. Chem.*, 872 (2004).
[45] B. Zhang, H.Z. Kou, Y. He, H.G. Wang, A.L. Gui. *Acta Crystallogr.*, **C60**, m341 (2004).
[46] P.D.W. Boyd, C.E.F. Rickard. *Acta Crystallogr.*, **E62**, m3200 (2006).
[47] A. Wolf, G.H. Shimer Jr, T. Meehan. *Biochemistry*, **26**, 6392 (1987).
[48] C.W. Jiang, H. Chao, H. Li, L.N. Ji. *J. Inorg. Biochem.*, **93**, 247 (2003).
[49] A.M. Pyle, J.P. Rehmann, R. Meshoyrer, C.V. Kumar, N.J. Turro, J.K. Barton. *J. Am. Chem. Soc.*, **111**, 3051 (1989).
[50] J.B. Le Pecq, C. Paoletti. *J. Mol. Biol.*, **27**, 87 (1967).
[51] Y.N. Xiao, C.X. Zhan. *J. Appl. Polym. Sci.*, **84**, 887 (2002).
[52] R. Indumathy, S. Radhika, M. Kanthimathi, T. Weyhermuller, B.U. Nair. *J. Inorg. Biochem.*, **101**, 434 (2007).
[53] O. Stern, M. Volmer. *Z. Phys.*, **20**, 183 (1919).
[54] S. Mahadevan, M. Palaniandavar. *Inorg. Chem.*, **37**, 693 (1998).
[55] M.T. Carter, M. Rodriguez, A.J. Bard. *J. Am. Chem. Soc.*, **111**, 8901 (1989).
[56] M. Rodriguez, A.J. Bard. *Anal. Chem.*, **62**, 2658 (1990).
[57] M.T. Carter, A.J. Bard. *J. Am. Chem. Soc.*, **109**, 7528 (1987).
[58] S. Satyanarayana, J.C. Dabrowiak, J.B. Chaires. *Biochemistry*, **31**, 9319 (1992).
[59] L. Jin, P. Yang. *J. Inorg. Biochem.*, **68**, 79 (1997).
[60] Y. Li, Y. Wu, J. Zhao, P. Yang. *J. Inorg. Biochem.*, **101**, 283 (2007).